J Polym Environ (2016) 24:343–355
DOI 10.1007/s10924-016-0780-9

ORIGINAL PAPER

Itaconic Acid Grafted Starch Hydrogels as Metal Remover: Capacity, Selectivity and Adsorption Kinetics

Diana Soto[1] · José Urdaneta[1] · Kelly Pernia[1] · Orietta León[1] · Alexandra Muñoz-Bonilla[2] · Marta Fernández-García[2]

Published online: 2 June 2016

Abstract Hydrogels were synthesized by free radical graft copolymerization of itaconic acid (IA) onto corn starch (S-*g*-IA). For this purpose, potassium permanganate ($KMnO_4$)-sodium bisulfite ($NaHSO_3$) was used as redox initiation system. The formation of grafted starches was confirmed by Fourier transform infrared spectroscopy, wide angle X-ray scattering, thermogravimetric analysis and scanning electron microscopy. The effect of monomer concentration, neutralization, addition of crosslinking agent, N,N-bismetilenacrilamide (MBAm), and initiator concentration on grafting efficiency and adsorption capacity of the starch hydrogels was investigated. It was demonstrated that the introduction of carboxyl and carbonyl groups promoted starch hydration and swelling. Grafting degree increased with the decrease of monomer concentration, increase of initiator concentration, grade of neutralization and the addition of MBAm without neutralization. Remarkably the resulting materials exhibited water absorption capacities between 258 and 1878% and the ability to adsorb metal ions. It was experimentally confirmed the metal uptake, obtaining the higher adsorption capacity ($q_e = 35$ mg/g) for the product prepared with the pre-oxidation and lower initiator concentration. The removal capacity order was $Pb^{2+}>Ni^{2+}>Zn^{2+}>Cd^{2+}$. Moreover, the experimental kinetic and the equilibrium adsorption data for Ni^{2+} and Pb^{2+} were best fitted to the pseudo-second order and Freundlich isotherm models, respectively. This work describes for the first time the preparation of metal removal hydrogels based on starch and itaconic acid using the pair redox system $KMnO_4$/$NaHSO_3$, which avoids the starch hydrolysis and allows itaconic acid grafting incorporation without the requirement of more reactive comonomers.

Keywords Starch · Itaconic acid · Grafting, Crosslinking · Hydrogels · Kinetics · Heavy metals

Introduction

Heavy metals, due to their high toxicity, present a serious threat to flora and fauna. These metals, coming from industry or urban wastewater, produce the degradation of environment; [1] therefore, their removal is mandatory. The common treatments to remove metal ions from contaminated waters are mostly based on chemical precipitation, ion-exchange, adsorption, membrane filtration, coagulation–flocculation, flotation and electrochemical methods [2]. Most of these techniques require elevated energy; e.g. electroflotation methods. Precipitation and electrochemical processes present also several disadvantages, which include incomplete metal removal (amounts in the range 1–100 mg/L) and great sludge generation [3]. Membrane filtrations, ion-exchange among other are expensive. In this sense, the search for new products from natural resources, mainly polysaccharides, for metal remediation is not only indispensable but also beneficial [4–7]. These products can be biodegradable,

✉ Orietta León
orleon@fing.luz.edu.ve

✉ Marta Fernández-García
martafg@ictp.csic.es

[1] Laboratorio de Polímeros y Reacciones, Escuela de Ingeniería Química, Facultad de Ingeniería, Universidad del Zulia, Sector Grano de Oro, Avenida 16 (Guajira), Ciudad Universitaria Dr. Antonio Borjas Romero, Edificio Petróleo y Química, Maracaibo 4011, Venezuela

[2] Departamento de Química y Propiedades de Materiales Poliméricos, Instituto de Ciencia y Tecnología de Polímeros (ICTP-CSIC), C/Juan de la Cierva 3, 28006 Madrid, Spain

cost-effective and nontoxic and can be used for agrochemicals release without risk of contamination or soil deterioration [4, 8, 9]. However, they can be low resistant to scratch, exhibit poor solubility, low mechanical properties, and instability at high temperatures and pHs during processing and with high tendency to retrogradation, expelling the water from the network. Nevertheless, these inconvenient can be overcome by chemical modification of the native polysaccharides.

It is well-known that one of the most abundant naturally occurring biopolymers is starch. It has diverse applications in areas of food, pharmaceuticals, textile, paper, and biomedical devices [10–14]. However, native starch can only show their water retention capacity but not efficient removal capacity for heavy metal ions [15]. One of the explored ways to improve this material is by radical copolymerization with vinyl monomers, such as acrylic acid, acrylamide among others [16–26]. Itaconic acid, another natural compound obtained from algae fermentation, has been widely used to modify natural products such as chitosan, alginate, cellulose, sisal [27–30] as well as starch [31–34]. To the best of our knowledge only one reported article dealing with the grafting copolymerization of itaconic acid with acrylamide as comonomer onto *cassava* starch using a redox system of ammonium persulfate (APS) and N,N,N′,N′-tetramethylethylenediamine (TEMED) to give pH responsiveness to the final superabsorbent hydrogel has been described [31]. The same group used in a previous work simultaneous irradiation technique for grafting polymerization of acrylic acid and acrylamide using gamma-rays as the initiator source [35]. None of these works use mild redox system avoiding the possibility of starch hydrolysis and therefore, the disablement of material. Besides they do not describe the grafting of itaconic acid using only this monomer.

Hebeish et al. [36] described the oxidation of starch using $KMnO_4$ in presence of different reductants such as citric acid, oxalic acid and sodium sulphite, under various conditions of pH, temperature, time, and permanganate concentration. Later, they reveals [37] that potassium permanganate acts as initiator for polymerization of acrylonitrile monomer (AN) and as oxidizing agent for starch on the graft copolymerization of AN onto starch. Zhang et al. [16, 38, 39] also reported the use of potassium permanganate with citric acid, sulfuric acid, as initiator systems of graft copolymerization. They reported that Mn^{+7} is applied to the graft copolymerization, it directly oxidizes the hydroxyl groups on the polysaccharide backbone to form radicals, which can initiate the monomer to graft onto the backbone. The main drawback of this reaction is that some radicals on the backbone can have chain-transfer reactions onto the monomer, which can lead to the formation of the homopolymer. In this case, these two reactions, homopolymerization and copolymerization, are competitive, being more probable the graft copolymerization; while if peroxides are used as initiators, both reactions are taking place simultaneously.

Having in mind all the mentioned above, this article describes the starch modification by grafting polymerization of itaconic acid using $KMnO_4/NaHSO_3$ as initiator system to create a superabsorbent hydrogel able to efficiently remove heavy metals. Experimental parameters such as monomer content, neutralization degree, crosslinking agent, and initiator concentration were varied to obtain hydrogels for effective heavy metal removal. These hydrogels were structural and thermally characterized by FTIR, WAXS and TGA. Swelling behavior was also analyzed as a function of pH. Heavy metals removals for the different itaconic acid grafted starches were investigated individually or in combination with the other metals to analyze their selectivity. In addition, the equilibrium adsorption and the experimental kinetic data for selected systems were studied using Freundlich isotherm and pseudo-second order models, respectively.

Experimental

Materials

Native corn starch (NS) used was food grade obtained from Alfonso Rivas & Cía. Itaconic acid ($C_3H_4(COOH)_2$, ≥99.9%, Merck) and N,N-methylene bis(acrylamide) (MBAm, 99%, Sigma-Aldrich) were used without purification. Hydrochloric acid (HCl, 37%), nitric acid (HNO_3, 65%), sodium chloride (NaCl, 99%), silver nitrate ($AgNO_3$, >99.9%), lead (II) nitrate ($Pb(NO_3)_2$, 99%), potassium permanganate ($KMnO_4$, 99%) nickel(II) sulfate ($NiSO_4.6H_2O$, 99 %) were purchased from Fisher Scientific as used as received. Ammonia solution (NH_4OH, 95%), iodine (I_2, 99.9%); and potassium iodide (KI, 100.5%) from J.T. Baker; hydroxylamine hydrochloride ($NH_2OH{\cdot}HCl$, 99%) and zinc sulfate ($ZnSO_4{\cdot}7H_2O$, 99.5%) from LabChemie were used as received. Phosphoric acid (H_3PO_4, ≥85%), monosodium phosphate (NaH_2PO_4, ≥98%), trisodium phosphate ($Na_3PO_4{\cdot}12H_2O$, ≥98%), sodium hydroxide (NaOH, 99%), cadmium(II) nitrate ($Cd(NO_3)_2{\cdot}4H_2O$, 99%) from Sigma-Aldrich; disodium hydrogen phosphate (Na_2HPO_4, 98%) from Scharlau; sodium bisulfite ($NaHSO_3$, 66.9%) from Mallinckrodt Baker; ethanol (C_2H_5OH, 99.9%) from Merck, potassium bromide (KBr, 99.5%) from Riedel-de-Haen; were all used as received.

Preparation of Starch Hydrogels

An aqueous dispersion of corn starch with a concentration of 0.6173 M of anhydroglucose units (AGU) (10 g of

starch in 100 mL distilled water) was prepared. The dispersion was introduced into a three-necked flask and heated at 75 °C for 15 min with gentle agitation. To this dispersion, 200 mL of water were added and cooled down to 60 °C. Then, the established amount of initiator and activator were added to polysaccharide, and the slurry was kept in contact with $KMnO_4$ (8×10^{-2} M) for 10 min. After this pre-oxidation step, IA monomer (neutralized at 70, 75 and 80% with NaOH or not neutralized), previously dissolved in a volume of 180 mL of distilled water, and MBAm crosslinking agent (only when no neutralized IA was used or neutralized at 75%) were added. Immediately, the final volume was increased up to 500 mL with distilled water and allowed to react for 3 h. Then, the mixture was cooled down and precipitated with ethanol to obtain the modified starch. Finally, the products were washed several times thoroughly with a mixture of 50 % v/v ethanol/water to remove any possible residual monomer and starch soluble fragments. The samples were dried in an oven at 40 °C until constant weight.

Materials Characterization

Infrared spectra of dry samples were obtained using FTIR Shimadzu IR Prestige equipment in KBr pellets.

Sol and gel fractions, F_{sol} and F_{gel}, were determined by the Lugol test [40]. Those parameters are defined as follows:

$$F_{sol}=\frac{m_i-m_f}{m_i} \quad (1)$$

$$F_{sol}=\frac{m_i-m_f}{m_i} \quad (2)$$

where m_i is the initial sample weight and m_f is the dry sample after immersion in distilled water at 60 °C during 24 h, and then Lugol test was performed. Determination of carboxyl group content was done following the modified procedure of Chattopadhyay et al. [41]. The mixture of 0.2 g of starch and 2.5 mL of HCI 0.1 N was discreetly stirred for 30 min. Then, it was filtered through a Whatman® qualitative filter paper (Grade 4) and washed with distilled water until no chlorine was detected. The starch was then transferred into a 50 mL beaker, and 30 mL of distilled water was added. Subsequently, the mixture was refluxed during 15 min for the complete starch gelatinization. After that, the system was titrated with NaOH 0.01 N solution using phenolphthalein as indicator. Native starch was used as control and all the measurements were executed by triplicate.

Then, the resulting graft yield, expressed as m_{eq} -COOH/100 g starch, was calculated following the Mostafa equation: [42]

$$\text{Graft } (\%) = \frac{\text{Carboxyl } (\%)}{0.045} \quad (3)$$

Determination of carbonyl group content was carried out following a strategy described in the literature [43]. Starch (0.4 g) in 10 mL of water was transferred into a 50 mL beaker and heated at 100 °C until gelation; then, it was slowly cooled to 40 °C. The pH of the solution was adjusted at 3.2 with HCl 0.1 M and then, 1.5 mL of hydroxylamine hydrochloride was added. Then, the mixture was led at this temperature for 4 h and the excess of hydroxylamine hydrochloride was titrated with HCl 0.1 M to adjust at pH = 3.2. The test was performed by triplicate in each sample.

The WAXS profiles of starches were registered in the reflection mode at 25 °C in a Bruker D8 Advance diffractometer equipped with a Goebel mirror and a PSD (Vantec) detector. Cu-Kα radiation was used and the equipment was calibrated with various standards. A step scanning mode was employed for the detector, with a 2θ step of 0.024° and 0.2 s per step. The WAXS degree of crystallinity, f_c, was determined from deconvolution of X-ray profiles into crystalline diffractions and the amorphous halo. In all the analyzed hydrogels the amorphous peak was centered at 2θ of 30.0 ± 0.1°.

The thermogravimetric analysis was performed in TGA Q500 equipment (TA Instruments). The instrument was calibrated in temperature and in weight by standard methods. Dynamic experiments were performed under inert atmosphere at heating rate of 10 °C/min in the temperature range between 40 and 800 °C. The average sample size was ca. 5 mg and the dry nitrogen flow rate was 20 cm^3/min. The decomposition activation energy (E_a) of samples was calculated by Broido method [44]. In addition, the thermograms were used to estimate the graft degree [31] of the samples according to the following equation:

$$\%\,\text{Grafting} = \frac{\sum \text{Weight loss on the 2nd stage} \times 100}{\sum \text{Weight loss on the 3rd stage}} \quad (4)$$

Scanning electron microscopy (SEM) characterization of starches was performed using Phillips XL30 equipment working at 25 kV and Au/Pd (80/20) coated samples.

Water adsorption behavior was measured by gravimetry using the tea-bag procedure described by Kabiri et al [45, 46]. Dried sample, m_s, 50 mg, placed in a tea bag was immersed in aqueous solution at different pHs, ranging from 2 to 11. The water uptake (H) was measured at different time intervals using the following equation:

$$H(\%) = \frac{m_{fh}-m_{ih}-F_c}{m_s}\times 100 \quad (5)$$

$$F_c = \frac{\sum_{i=1}^{n} (m_{bh} - m_b)_i}{n} \quad (6)$$

where m_{ih} and m_{fh} are the initial and final weight including the tea bag, respectively, and F_c is the correction factor for the possible adsorption from the tea bag; being m_b and m_{bh} the weight of dry and wet tea bag, respectively, and n the number of replications ($n = 5$).

Atomic absorption spectrometer Perkin Elmer PE 3030 was used to follow the ability of starches to adsorb metal ions from the amount of residual metal ion in the solution. Ion aqueous solutions of Pb^{2+} (0.37 mmol/L), Cd^{2+} (0.90 mmol/L), Zn^{2+} (1.52 mmol/L), and Ni^{2+} (1.70 mmol/L) were prepared in a total concentration of 100 mg/L. To 25 mL of each ion solution, 50 mg of polymer were added and, previous to adsorption experiments, slowly and gently shook during 24 h at slow rate and at room temperature. Likewise, the effect of pH variation on the adsorption ability of samples in water solutions was also evaluated for Ni^{2+} and Pb^{2+} ions. The pH values of 2.5, 3.5 and 4.5 in the solutions were obtained by adjusting with H_2SO_4 and HNO_3 0.01 M. The adsorption isotherms were measured at 15, 30 min, 1, 2, 4 and 24 h.

Results and Discussion

Preparation of Grafted Starch Hydrogels

Graft polymerizations of IA onto starch, S-*g*-IAx, were performed by free radical polymerization using $KMnO_4$/$NaHSO_3$ redox system as initiator ([I] = 8×10^{-3} M). As mentioned above, this redox system does not hydrolyze the starch and is suitable for the copolymerization reaction. In Table 1 are collected the percentage of carbonyl and carboxyl groups of the samples obtained at the different reaction conditions as well as the monomer and initiator concentrations used in each reaction.

From the carbonyl content it can be established that the starch was effectively pre-oxidized and the graft reaction occurred throughout the intermediate aldehyde starch. Interestingly, the carboxyl groups decreases as monomer concentration increases (S-*g*-IA_0.42[IA], S-*g*-IA_0.66[IA] and S-*g*-IA_1[IA]) from 0.24 to 0.12. This decrease of carboxyl groups is more pronounced when the monomer is neutralized (S-*g*-IA_70 N, S-*g*-IA_75 N and S-*g*-IA_80 N). The same occurs when the cross-linked agent is used. However, when the ratio of initiator is 3/4 of the initial, named S-*g*-IA_3/4[I] (6×10^{-3} M), an increment of groups is produced. Moreover, when is initiator concentration is half of initial concentration, named S-*g*-IA_1/2[I], the amount of these groups decreases with respect to the previous one but is still higher than the percentage of the grafted starch with the initial initiator concentration of 8×10^{-3} M, S-*g*-IA_1[IA]. Nevertheless, in all the cases, the carboxyl content increases in comparison to native starch, indication of graft polymerization. Comparatively, the carboxyl content is higher when MBAm is incorporated, named CL when no neutralized monomer is used and CL-75 N when the monomer is neutralized at 75 %, in comparison with S-*g*-IA_75 N. In the first case is 0.14 against 0.12 and in the second is 0.12 against 0.09, see Table 1.

Characterization of Graft Copolymers

Itaconic acid grafting into native starch was analyzed by FTIR measurements (see Fig. 1a). The characteristic regions, i.e. the fingerprint region, 800–1500 cm^{-1}, the C–H stretch region between 2800 and 3000 cm^{-1}, and finally the O–H stretch region between 3000 and 3600 cm^{-1} are observed. Starches also exhibited complex vibrational modes at low wavenumbers (below 800 cm^{-1}) due to the skeletal mode vibrations of the glucose pyranose ring. The band at 1640 cm^{-1} characteristic of water adsorbed in the amorphous regions of starch [47] is observed as well as a small shoulder around 1730 cm^{-1} due to carboxylic acid C=O stretching and ca. 1630 cm^{-1} corresponding to C–O–H in-plane bending due to itaconic acid grafting.

Figure 1b shows the WAXS profiles of native starch and grafted starch synthesized using half of the initial initiator concentration and 500 mL of volume of pre-oxidation instead of 300 mL, named S-*g*-IA_1/2[I]b. It is easily observed the A-type crystalline structure of NS, typically found on cereal starches [10, 48]. The pattern reveals the characteristic peaks of this structure with strong reflections at 2θ about 15° and 23°, and an unresolved doublet at 2θ = 17° and 18° [48–51]. The relative percentage of crystallinity [34] previously calculated by our group for NS, 28.3 %, slightly varies with the incorporation of itaconic acid monomer, giving rise to an increment of the amorphous phase. The peaks appear broader and gentler after grafting process, indicating the loss of crystallinity [52–54]. The hydrogen bonds between molecules are weakened and, thus, the thermoplasticity of IA grafted starches increased. As mentioned, the crystallinity of grafted copolymer decreases up to 22 %. The grafting reaction disrupts the intra- and intermolecular bonds between hydroxyl groups present on the starch, which are the responsible of the crystalline structure of NS [13, 55, 56]. However, the incorporation of itaconic acid does not completely destroy the crystalline structure of starch. Besides, the broad peak located near 20°, which can be attributed to V-type (single helix) structures of amylose, seems to be more noticeable due to the decrease of A-type crystal structure.

Figure 2 shows the microscopy analysis of native starch as well as grafted copolymers. Native starch presents a

Table 1 Carbonyl and carboxyl contents of the modified starches

Sample	[IA] (M)	[KMnO4][a] × 10^3 (M)	Carbonyl content* (%CO)	Carboxyl content* (%COOH)
NS	–	–	0.80 ± 0.03	0.05 ± 0.01
S-g-IA_0.42[IA]	0.077	8.0	0.15 ± 0.01	0.24 ± 0.01
S-g-IA_0.66[IA]	0.122	8.0	0.10 ± 0.02	0.16 ± 0.01
S-g-IA_1[IA]	0.185	8.0	0.07 ± 0.01	0.12 ± 0.01
S-g-IA_70 N	0.185	8.0	0.08 ± 0.01	0.17 ± 0.01
S-g-IA_75 N	0.185	8.0	0.02 ± 0.01	0.09 ± 0.01
S-g-IA_80 N	0.185	8.0	0.08 ± 0.02	0.08 ± 0.01
CL	0.185	8.0	0.07 ± 0.01	0.14 ± 0.01
CL-75 N	0.185	8.0	0.06 ± 0.01	0.12 ± 0.01
S-g-IA_3/4[I]	0.185	6.0	0.18 ± 0.01	0.26 ± 0.02
S-g-IA_1/2[I]	0.185	4.0	0.12 ± 0.01	0.17 ± 0.01
S-g-IA_1/2[I]b	0.185	4.0	0.11 ± 0.01	0.12 ± 0.01

Volume of pre-oxidation = 500 mL for S-*g*-IA_1/2[I]b

[a] [KMnO4]/[NaHSO3] = 2.5 in all cases

* Before lixiviation

bimodal distribution of grains, typical from cereal starches, with medium particle size ranging from 10 to 20 μm and small sizes from 5 to 10 μm [57–59]. The granules are smooth and irregular, varying from spherical to polygonal, with higher proportion of the latest, which is characteristic of corn starch [59, 60]. In the case of grafted copolymers, i.e. S-*g*-IA_1/2[I]b and S-*g*-IA_3/4[I], there are considerable changes in the morphology of these grains, indicating the modification process [61, 62]. The aggregation of granules because of the binder of hydroxyl groups, to form hydrogen and covalent bonds between starch chains, allows the formation of adequate pores for water absorption [62].

Thermal Behavior

The thermal behavior of starches was studied by thermogravimetric analysis. In Fig. 3 the degradation curves carried out at 10 °C/min under inert nitrogen atmosphere of NS and S-*g*-IA_3/4[I] grafted copolymer are displayed. As occurs in polysaccharides, there are two different stages clearly observed; the first one corresponds to the loss of water associated to its hygroscopic character, and the second step corresponds to the depolymerization of natural polymer with mainly elimination of water and CO_2 [31, 56, 63–65]. The sharp peak found in NS is also found in the grafted starches. However, it is also observed the presence of a small step at lower temperatures. This corresponds to the decarboxylation reaction of grafted poly(itaconic acid), which exhibits low stability [27–29]. In spite of this, the grafting is not enough to completely destabilize the starch main chain. The main peak of degradation is observed with a slightly shift to higher temperatures, (see also Table 2).

Considering the equation of Broido [44] as:

$$\ln\left[\ln(w_0 - w_\infty)/(w - w_\infty)\right] = -(Ea/RT) + \text{constant} \quad (7)$$

where E_a is the activation energy and w is the sample weight at defined time, while w_0 and w_∞ are the initial and final weights, respectively. From the slope of the logarithmic representation of these parameters, the activation energy can be determined. The thermal degradation process of modified starches is less favorable than in native starch, probably as a consequence of the increase of carboxyl groups' content (see E_a values in Table 2) [66]. Therefore, the incorporation of itaconic acid gives globally more stability to the starch.

Water Uptake Behavior

The results of water uptake behavior of copolymers in water and saline solutions as a function of grafting degree and gel fraction are collected in Table 3. In water, the hydrogels with higher swelling capacity are those obtained with lower initiator concentration (S-*g*-IA_1/2[I]) and with lower initiator and reactant contents in the pre-oxidation step (S-*g*-IA_1/2[I]b). The crystallinity disruption, therefore, the increase of amorphous regions after grafting reaction favors the water uptake [67]. The lowest values are found for copolymers with lower concentration of IA, i.e. S-*g*-IA_0.42[IA] and S-*g*-IA_0.66[IA], showing an increment of swelling with the monomer concentration as well as with the diminishment of grafting. This is because itaconic acid is a diprotic acid, so high degrees of grafting implies an increase of possible inter and intramolecular hydrogen bonds, e.g. high crosslinking, which impedes the swelling. Likewise, the decrease on initiator concentration

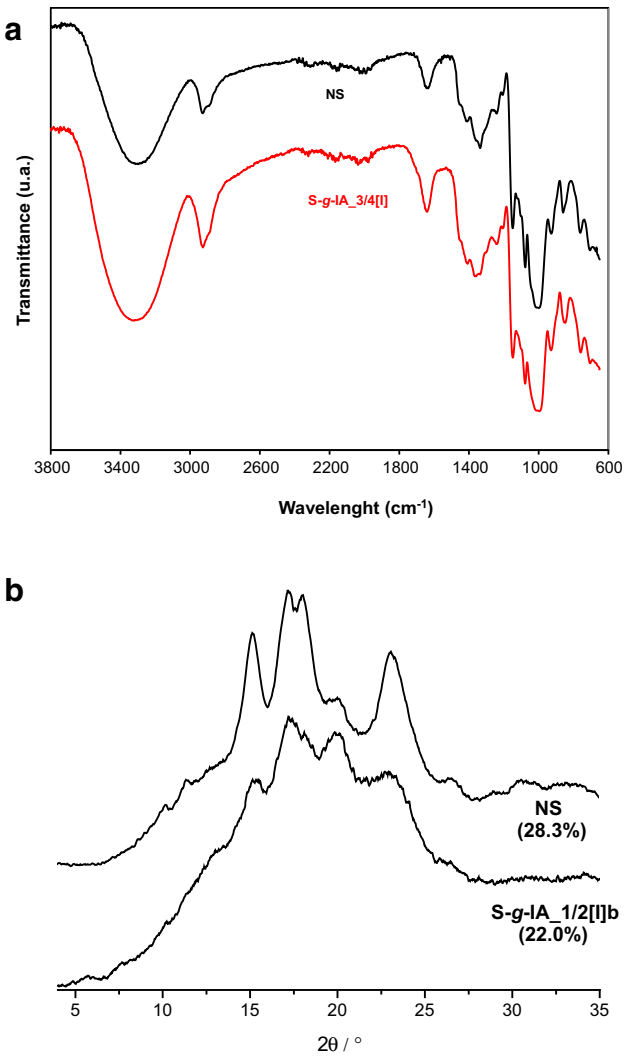

Fig. 1 **a** FTIR spectra and **b** WAXS profiles of native and S-*g*-IA_1/2[I]b starches, respectively

causes diminishment on the grafting degree, so an increase on the water uptake capability. The preparation of copolymer in a large volume, S-*g*-IA_1/2[I] versus S-*g*-IA_1/2[I]b, generates a competition between grafting and crosslinking reactions, provoking an increase of water sorption.

Next, the neutralization effect was evaluated, revealing that the increase provokes similar or higher gel fractions, which means that the hydrolysis is not favored. Moreover, the neutralization allows reaching higher values of water uptake. On the contrary, the introduction of crosslinking agent, MBAm, to the reaction, samples CL and CL-75 N, produces a decrease on the gel fraction and degree of grafting, increasing the starch hydrolysis. Specifically, higher water uptake is achieved for S-*g*-IA_1[IA] in comparison with CL. In the case of neutralized samples, S-*g*-IA_75 N, its swelling behavior is greater than that of CL-75 N as well as its gel fraction (93.0 vs. 72.8 %) and grafting degree (2.1 vs. 1.5 %).

As summary, it can be said that these copolymers present a polyelectrolyte behavior in water. This performance is also found in the majority of grafted starches in saline solution, since the increment of ionic strength exerts a reduction on water uptake ability. However, the contrary effect is clearly observed when the monomer concentration augments, S-*g*-IA_0.42[IA], S-*g*-IA_0.66[IA] and S-*g*-IA_1[IA], that is the water uptake increases. This may be due to an exchange between Na^+ cations and H^+ protons of hydrogel, which allows higher water content to be introduced.

Figure 4 displays the kinetics of water uptake of all the obtained systems. In all the cases, the swelling equilibrium is reached after ca. 2 h. However, anomalous swelling behavior is found in some copolymers. At the beginning of the swelling process, the curves exhibit a maximum in the water uptake after which the swelling gradually decreases to an equilibrium value at longer times. This is described in the literature as the overshooting effect [68–70]. Initially, this effect was described taking into account the glassy state of the polymer, which induces a moving rigid core during swelling [71, 72]. Moreover, the kinetic was also interpreted as a consequence of an autocatalytic process of the water penetration into the gel. Other authors established that the overshooting effect might be a consequence of a

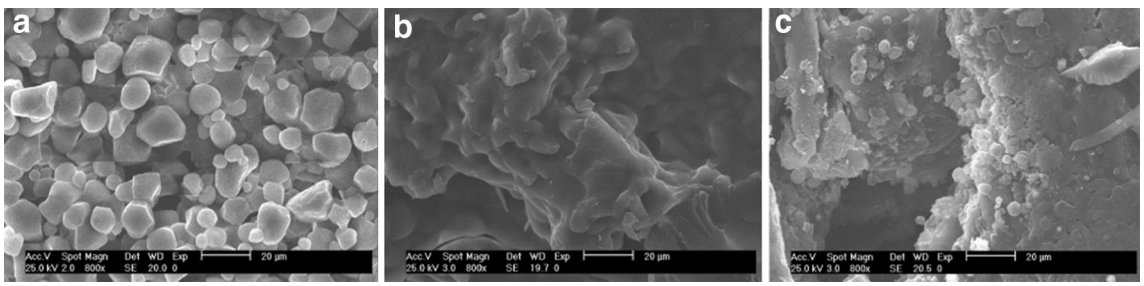

Fig. 2 SEM micrographs of **a** native starch; **b** grafted copolymer S-*g*-IA_1/2[I]b and **c** grafted copolymer S-*g*-IA_3/4[I] at a magnification of 800×

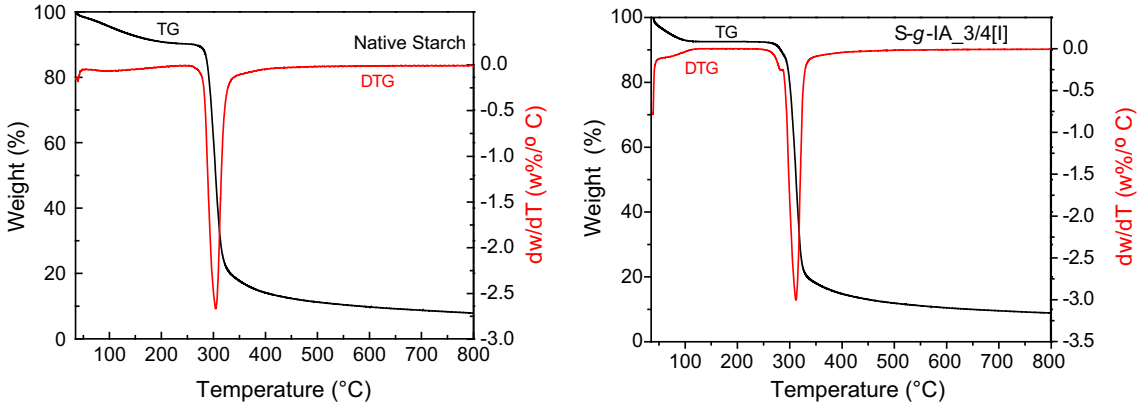

Fig. 3 TGA and DTG profiles of NS and S-*g*-IA_3/4[I] starch

Table 2 Thermogravimetric parameters of native starch and S-g-IA_3/4[I] grafted copolymer

Sample	T_{onset1} (°C)	T_{onset2} (°C)	T_{max1} (°C)	T_{max2} (°C)	Chart at 800 °C (%)	E_a (kJ/mol)
NS	–	288	–	304	7.9	184
S-g-IA_3/4[I]	278	296	283	313	8.9	262

Table 3 Values of gel fraction, grafting degree and swelling behavior at the equilibrium, H^{∞}, in water and saline solutions

Copolymer	Gel fraction (%)	Grafting[a] (%)	H^{∞} in water (%)	H^{∞} in saline (%)
S-*g*-IA_0.42[IA]	42.2	2.6	258	370
S-*g*-IA_0.66[IA]	78.0	2.5	413	824
S-*g*-IA_1[IA]	78.8	2.1	905	1541
S-*g*-IA_70 N	88.4	2.3	528	323
S-*g*-IA_75 N	93.0	2.1	1217	315
S-*g*-IA_80 N	92.6	2.6	1824	407
CL	84.5	2.2	611	603
CL-75 N	72.8	1.5	777	114
S-*g*-IA_3/4[I]	53.3	2.1	1424	556
S-*g*-IA_1/2[I]	76.00	2.0	1562	1181
S-*g*-IA_1/2[I]b	90.0	1.8	1878	610

[a] Values obtained for the gel fraction

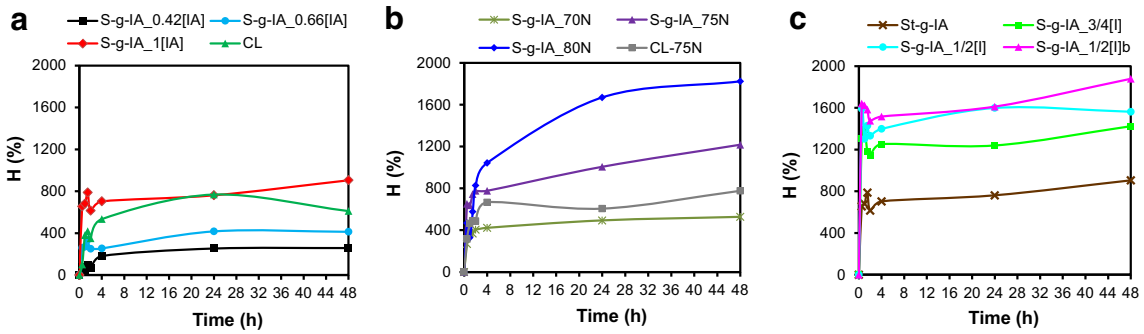

Fig. 4 Swelling kinetics of obtained systems. **a** Represents the copolymers obtained with different monomer concentration and also with the addition of MBAm crosslinker agent; **b** the monomer type and the percentage of neutralized monomer; and **c** the different initiator concentration used

spontaneous rearrangement of the gel structure on the dynamic swelling [69]. Recently, the phenomenon was also observed in acid solution where pH is lower than pK_a of hydrogels obtained by graft crosslink copolymerization of sodium alginate (SA) and acrylic acid (AA) using MBAm as crosslinker. This effect is interpreted as a cooperative physical crosslinking caused by the hydrogen bond formation between the carboxyl groups of the hydrogels in a hydrophobic environment [70]. As can be observed in Fig. 4a the swelling increases as concentration of monomer does. Likewise, the increase on neutralized monomer provokes an augment on the water uptake ability (see Fig. 4b). Figure 4c represents the swelling curves of copolymers as a function of initiator concentration, showing a decrease on the water adsorption capacity as the initiator concentration increases.

Subsequently, the effect of pH on the swelling behavior was studied. As an example, Fig. 5 represents H^{∞} in water for S-*g*-IA_1/2[I]b, S-*g*-MA_75 N and S-*g*-MA_80 N copolymers as a function of pH at room temperature. At low pH values the maximum of water uptake is low because there is an increment on the protonation of carboxylic groups; whereas the uptake is higher when the pH increases above pK_a. The number of charges increases in the network, generating anionic units, which induce electrostatic repulsions within macromolecular chains. This fact produces a higher expansion of the network and then, of the swelling ability [70, 73, 74]. In the case of grafted copolymers with neutralized monomer, there is also a maximum near neutral pH, but after it the hydrogel shrinks. This is because the ionization of the ionizable component is completed and then, the swelling process stops. Thus, the pH augment only increases the ionic strength [75].

Heavy Metal Adsorption

The ability of these itaconic acid grafted starches to remove heavy metals from aqueous solutions was evaluated by atomic absorption spectrometry. The amount of Cd^{2+}, Ni^{2+}, Pb^{2+} and Zn^{2+} ions retained by the material expressed as the ratio of adsorbate mass per adsorbent mass, q_e, as well as values of the partition coefficient, k_d, and the retention capacity, Q_r, was determined in all the samples, and the results are collected in Table 4. Metal adsorption becomes regulated by the ion charge, hydrodynamic radius and the characteristics of the material and normally the hydration is inversely related to the ionic radius and this follows $Pb^{2+}>Cd^{2+}>Zn^{2+}>Ni^{2+}$.

Interestingly, the removal capacity of copolymer increases as higher amount of itaconic acid is grafted [15]. The copolymers with higher removal capacity are those with lower concentration of initiator, S-*g*-IA_1/2[I]b, which also presents the highest swelling capacity. On the contrary, the lowest found values are for S-*g*-IA_1[IA] with 8.4 mg/g in the removal of Zn^{2+} and 8.2 mg/g for Cd^{2+}. The removal activity is related to the material crosslinking, the amount and disposition of acid groups, among other factors related to the nature and properties of adsorbent.

Another parameter that influences the ability to remove metals is the pH medium because the pH of the solution determines the ionic state of the metal as well as of the functional groups at the surface of adsorbent [76–78]. In this work, the capacity of remotion as a function of pH was studied for two ions, nickel and lead, and three copolymers (S-*g*-IA_1[IA], S-*g*-IA_80 N and S-*g*-IA_1/2[I]b, which present proper suitability as seen in Fig. 4. Figure 6 displays the amount of ions adsorbed per gram of S-*g*-IA_1[IA], S-*g*-IA_80 N and S-*g*-IA_1/2[I]b hydrogels as a function of pH. As expected, there is an increment on the ability to remove ions as increasing pH, since exists higher amount of ionized carboxylic groups able to adsorb larger amount of ions [79, 80]. It is also noticeable that in the near to itaconic acid pKa (~3.8), there is a slight slowdown in the uptake, due to there is the same concentration of carboxylate and carboxylic groups.

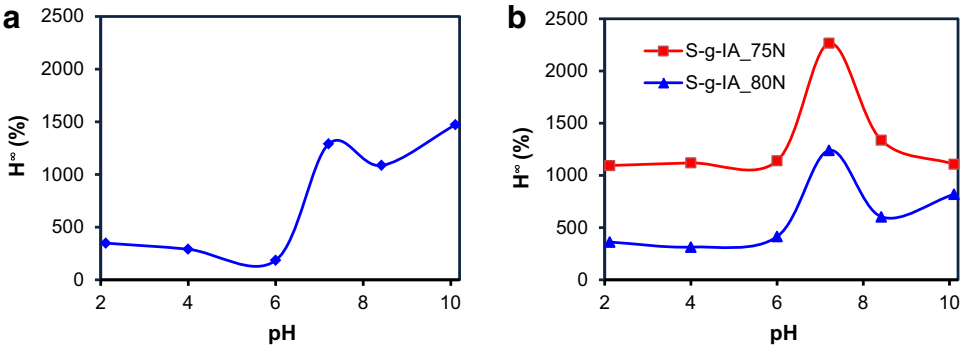

Fig. 5 Variation of maximum water uptake at the equilibrium as a function of pH of **a** S-*g*-IA_1/2[I]b and **b** S-*g*-MA_75N and S-*g*-MA_80 N starches

Table 4 Amount of removed metal ion per gram of copolymer, q_e, values of the partition coefficient, k_d, and the retention capacity, Q_r, for all the starches

Sample	q_e (mg of removed metal/g of hydrogel)				k_d				Q_r			
	Cd^{2+}	Ni^{2+}	Pb^{2+}	Zn^{2+}	Cd^{2+}	Ni^{2+}	Pb^{2+}	Zn^{2+}	Cd^{2+}	Ni^{2+}	Pb^{2+}	Zn^{2+}
NS	8.0	8.3	5.2	3.2	95.6	99.3	58.6	34.0	0.14	0.28	0.05	0.10
S-*g*-IA_0.42[IA]	9.0	13.1	16.2	13.3	109.0	176.7	238.8	180.3	0.16	0.45	0.16	0.41
S-*g*-IA_0.66[IA]	10.0	13.1	10.3	10.3	125.5	176.7	129.4	128.8	0.18	0.45	0.10	0.31
S-*g*-IA_1[IA]	8.2	18.5	27.9	8.4	97.8	293.0	633.6	101.4	0.15	0.63	0.27	0.26
S-*g*-IA_70 N	13.0	28.1	13.5	11.5	175.0	637.6	184.7	148.5	0.23	0.96	0.13	0.35
S-*g*-IA_75 N	10.5	18.8	26.4	11.5	132.8	301.0	561.4	148.5	0.19	0.64	0.26	0.35
S-*g*-IA_80 N	8.7	10.5	30.7	9.6	104.5	133.1	797.1	119.4	0.15	0.36	0.30	0.29
CL	10.4	14.7	29.1	12.1	130.5	207.3	697.4	158.7	0.18	0.50	0.28	0.37
CL-75 N	9.0	14.0	28.1	19.9	109.1	194.7	639.0	330.0	0.16	0.48	0.27	0.61
S-*g*-IA_3/4[I]	8.2	11.5	29.3	10.9	97.8	148.8	709.8	138.5	0.15	0.39	0.28	0.33
S-*g*-IA_1/2[I]	9.4	22.0	30.3	9.6	116.0	392.1	769.1	119.4	0.17	0.75	0.29	0.29
S-*g*-IA_1/2[I]b	8.7	13.4	35.0	10.9	104.5	182.7	1168.0	138.5	0.15	0.46	0.34	0.33

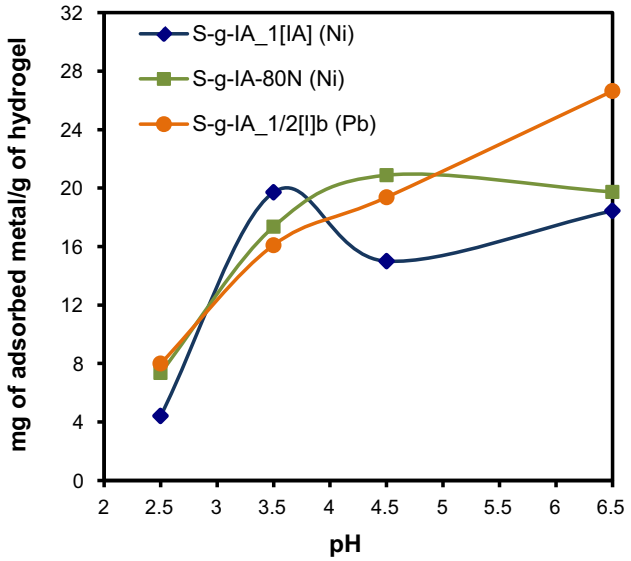

Fig. 6 The ability of S-*g*-IA_1[IA], S-*g*-IA_80 N and S-*g*-IA_1/2[I]b starches to remove nickel and lead as a function of pH

Competitive Adsorption of Metals

The selectivity of S-*g*-IA_1[IA], S-*g*-IA_80 N and S-*g*-IA_1/2[I]b for all the metals was measured in the same conditions that above and the metal amount in the solution after contact with each starch is depicted in Fig. 7. As can be observed, S-*g*-IA_80 N and S-*g*-IA_1/2[I]b follows the trend: $Pb^{2+}>>Ni^{2+}>Cd^{2+}>Zn^{2+}$ whereas S-*g*-IA_1[IA] presents this tendency $Pb^{2+}>>Zn^{2+}>Cd^{2}>Ni^{2+}$. In all the cases Pb^{2+} is the ionic specie more easily removed and that

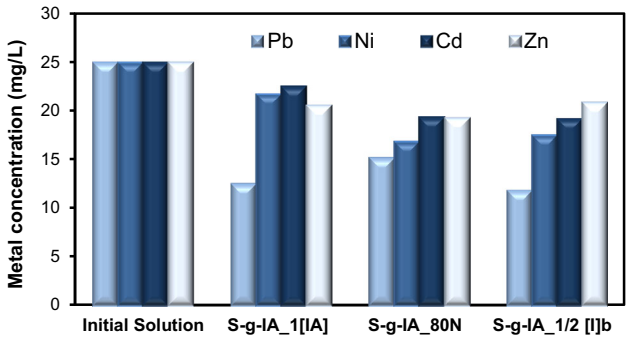

Fig. 7 Competitive adsorption studies of metals forS-*g*-IA_1[IA], S-*g*-IA_80 N and S-*g*-IA_1/2[I]b starch hydrogels

it follows the same trend that when only one metal is tested.

Isotherms and Kinetics of Adsorption

The equilibrium isotherms of adsorption are crucial to describe the interactions between analyte or adsorbate and sorbent. The respective sorption equilibrium are usually described by the well-known Langmuir or Freundlich relationships [81]. Freundlich equation, which is applied for multilayer adsorption on heterogeneous adsorbent and assumes that the adsorption sites increase exponentially with respect to the heat of adsorption, is described as $q_e = KC_e^{1/n}$. where K and $1/n$ are constants related to adsorption capacity and adsorption intensity, respectively. If the value of $1/n$ is higher than 1, the adsorption process is feasible and favorable [18].

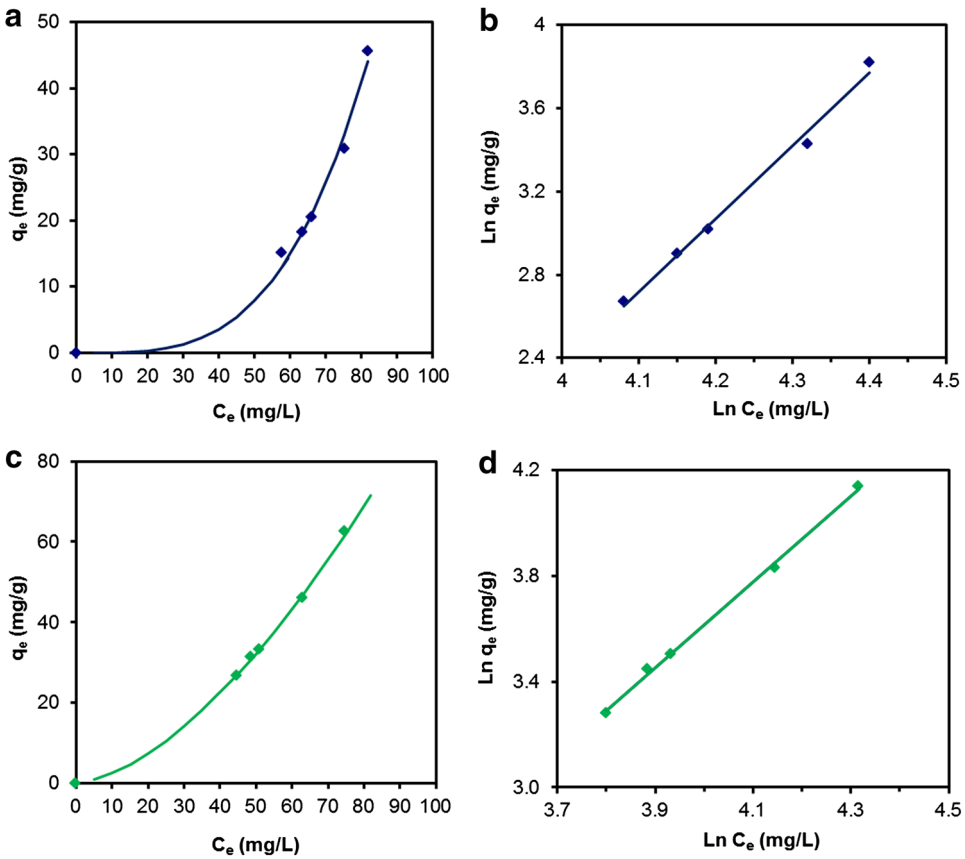

Fig. 8 Freundlich adsorption isotherms for **a**, **b** $Ni^{2+}$and **c**, **d** Pb^{2+}ions as a function of S-*g*-IA_80 N and S-*g*-IA_1/2[I]b concentrations, respectively

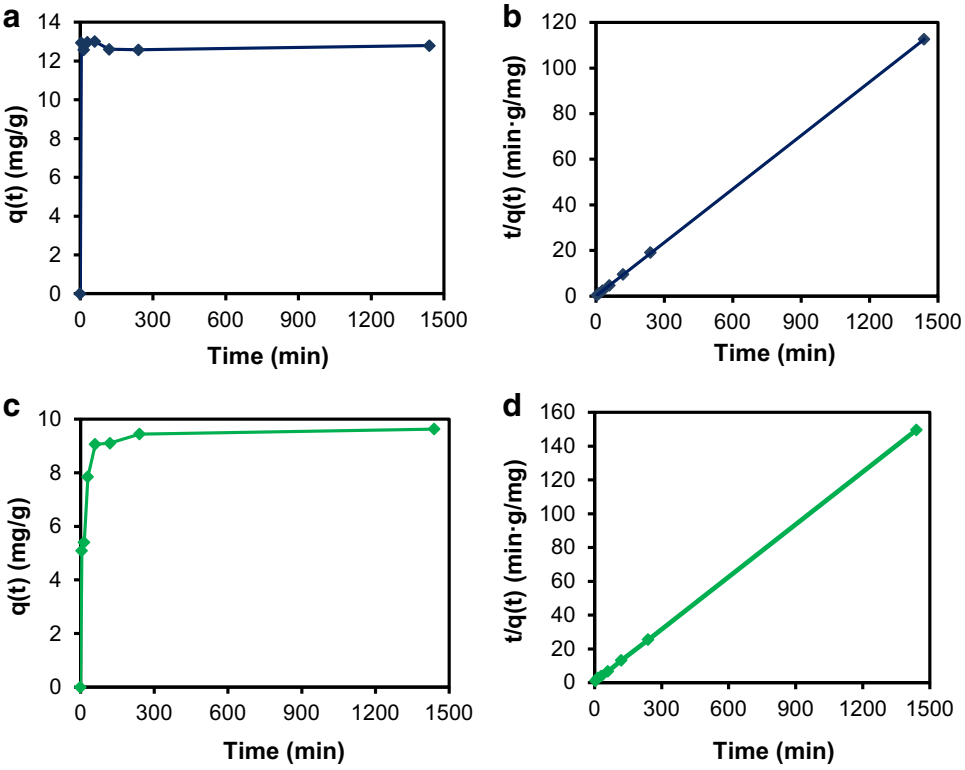

Fig. 9 **a**, **b** Adsorption curves versus time for Ni^{2+} using S-*g*-IA_80 N starch and **c**, **d** for Pb^{2+} with S-*g*-IA_1/2[I]b starch, respectively

In the present work, Fig. 8 represents, in their exponential and linear forms, the adsorption equilibrium for Pb^{2+} and Ni^{2+} ions as a function of S-*g*-IA_80 N and S-*g*-IA_1/2[I]b equilibrium concentrations (C_e), respectively. As it can be observed, both systems follow the Freundlich equation. Resulting values of K and 1/*n* of 8.7×10^{-6} $(mg/g)(L/mg)^{1/n}$ and 0.29 for Ni^{2+} and 56.5×10^{-3} $(mg/g)(L/mg)^{1/n}$ and 0.62 for Pb^{2+}, respectively, indicating that the adsorption processes in both systems are favorable.

Besides, adsorption time is an important parameter because this factor can reflect the adsorption kinetics of an adsorbent for a certain initial concentration of the adsorbate. The effect of adrption time on the adsorption curves of Pb^{2+} and Ni^{2+} ions by S-*g*-IA_80 N and S-*g*-IA_1/2[I]b, respectively, are represented in Fig. 9. The adsorption rate is very fast during the first 5 min of the process, during this period the respective removals of Ni^{2+} and Pb^{2+} are 12.9 and 5.1 mg/g for S-*g*-IA_80 N and S-*g*-IA_1/2[I]b, respectively. In both cases, after this period, the adsorption rate is slow down and adsorption equilibrium is gradually achieved within 50 min, in which the respective removals of Ni^{2+} and Pb^{2+} reached values of 12.9 and 9.6 mg/g for S-*g*-IA_80 N and S-*g*-IA_1/2[I]b, respectively. Both curves fit very well with the pseudo-second order kinetics (see plots 9B, 9D).This model [82] is based on the plotting of $t/q(t)$ against t (see the following equation), which should give a linear relationship, where t is time and $q(t)$ is the total adsorbed amount at time t.

$$\frac{t}{q(t)} = \frac{1}{k_2\left(q_e^C\right)^2} + \frac{t}{q_e^C} \tag{8}$$

In this case, q_e^C is treated as an adjustable parameter; this made possible to compare its values with the real values, and k_2 is the so-called pseudo-second order constant.

In the current work, k_2 calculated values are 0.11 g/mg min for Ni^{2+} and 1.5×10^{-2} g/mg min for Pb^{2+} adsorption. The q_e^C calculated values are 12.8 and 9.6 mg/g, while experimental obtained values are 12.8 and 9.7 mg/g, respectively for Ni^{2+} and Pb^{2+} adsorption processes. These values demonstrate the validity of this model and that the removal from a solution is due to physicochemical interactions between the metal ion and the starch, being the surface adsorption that involves chemisorption/quelation the rate-limiting step.

Conclusions

New hydrogels were obtained by graft copolymerization of starch with itaconic acid using mild redox conditions. The grafting was characterized by several techniques, such as FTIR, WAXS and TGA. The swelling behavior was enlarged with the increase of IA monomer content and the monomer neutralizing degree, without the crosslinking addition and with the diminishment of initiator and reactants in the pre-oxidation step. The water uptake of some of these grafted starches was around 1800 %. In addition, the swelling behavior showed pH dependence. These hydrogels were able to adsorb heavy metals with preference for lead, as follows $Pb^{2+}>>Ni^{2+}>Zn^{2+}>Cd^{2+}$. The experimental data was fitted to Freundlich adsorption isotherm and the pseudo-second order kinetic model. In summary, these biopolymeric materials based on starch and itaconic acid can be satisfactorily used as adsorbent for removal of water contaminants and their preparation does not require potent and contaminant redox systems.

Acknowledgments Authors thanks Consejo de Desarrollo Científico y Tecnológico (CONDES) of Universidad del Zulia for the financial support (Project VAC-CONDES-CC-0136-14). A. Muñoz-Bonilla thanks MINECO for her Ramon y Cajal contract.

References

1. Saeed A, Akhter MW, Iqbal M (2005) Removal and recovery of heavy metals from aqueous solution using papaya wood as a new biosorbent. Sep Purif Technol 45(1):25–31
2. Fu F, Wang Q (2011) Removal of heavy metal ions from wastewaters: a review. J Environ Manag 92(3):407–418
3. Bayramoglu G, Denizli A, Bektas S, Yakup Arica M (2002) Entrapment of Lentinus sajor-caju into Ca-alginate gel beads for removal of Cd(II) ions from aqueous solution: preparation and biosorption kinetics analysis. Microchem J 72(1):63–76
4. Vandenbossche M, Jimenez M, Casetta M, Traisnel M (2015) Remediation of heavy metals by biomolecules: a review. Crit Rev Environ Sci Technol 45(15):1644–1704
5. Bhat MA, Chisti H, Shah SA (2015) Removal of heavy metal ions from water by cross-linked potato di-starch phosphate polymer. Sep Sci Technol 50(12):1741–1747
6. Varghese LR, Das N (2015) Removal of Hg (II) ions from aqueous environment using glutaraldehyde crosslinked nanobiocomposite hydrogel modified by TETA and β-cyclodextrin: optimization, equilibrium, kinetic and ex situ studies. Ecol Eng 85:201–211
7. Kandile NG, Mohamed HM, Mohamed MI (2015) New heterocycle modified chitosan adsorbent for metal ions (II) removal from aqueous systems. Int J Biol Macromol 72:110–116
8. Jin SP, Wang YS, He JF, Yang Y, Yu XH, Yue GR (2013) Preparation and properties of a degradable interpenetrating polymer networks based on starch with water retention, amelioration of soil, and slow release of nitrogen and phosphorus fertilizer. J Appl Polym Sci 128(1):407–415
9. Campos EVR, de Oliveira JL, Fraceto LF, Singh B (2015) Polysaccharides as safer release systems for agrochemicals. Agron Sustain Dev 35(1):47–66
10. Tester RF, Karkalas J, Qi X (2004) Starch—composition, fine structure and architecture. J Cereal Sci 39(2):151–165
11. Sajilata MG, Singhal RS, Kulkarni PR (2006) Resistant starch–a review. Compr Rev Food Sci Food Saf 5(1):1–17
12. Nair SB, Jyothi AN (2014) Cassava starch-graft-polymethacrylamide copolymers as flocculants and textile sizing agents. J Appl Polym Sci 131(2):11

13. BeMiller JN, Whistler RL (eds) (2009) Starch: chemistry and technology, vol 3. Academic Press, London
14. Wang YJ, Jiang L, Duan JK, Shao SX (2013) Effect of the carbonyl content on the properties of composite films based on oxidized starch and gelatin. J Appl Polym Sci 130(5):3809–3815
15. Lu QL, Gao P, Zhi H, Zhao HY, Yang YP, Sun BW (2013) Preparation of Cu(II) ions adsorbent from acrylic acid-grafted corn starch in aqueous solutions. Starch-Starke 65(5–6):417–424
16. Zhang L, Gao J, Tian R, Yu J, Wang W (2003) Graft mechanism of acrylonitrile onto starch by potassium permanganate. J Appl Polym Sci 88(1):146–152
17. Lu S, Duan M, Lin S (2003) Synthesis of superabsorbent starch-graft-poly(potassium acrylate-co-acrylamide) and its properties. J Appl Polym Sci 88(6):1536–1542
18. Liu Y, Wang W, Wang A (2010) Adsorption of lead ions from aqueous solution by using carboxymethyl cellulose-g-poly (acrylic acid)/attapulgite hydrogel composites. Desalination 259(1–3):258–264
19. Zheng Y, Hua S, Wang A (2010) Adsorption behavior of Cu2+ from aqueous solutions onto starch-g-poly(acrylic acid)/sodium humate hydrogels. Desalination 263(1–3):170–175
20. Abd El-Rehim HA, Diaa DA (2012) Radiation-induced eco-compatible sulfonated starch/acrylic acid graft copolymers for sucrose hydrolysis. Carbohydr Polym 87(3):1905–1912
21. Tay SH, Pang SC, Chin SF (2012) Facile synthesis of starch-maleate monoesters from native sago starch. Carbohydr Polym 88(4):1195–1200
22. Kaur I, Sharma M (2012) Synthesis and characterization of graft copolymers of Sago starch and acrylic acid. Starch-Starke 64(6):441–451
23. Guo Q, Wang Y, Fan Y, Liu X, Ren S, Wen Y, Shen B (2015) Synthesis and characterization of multi-active site grafting starch copolymer initiated by $KMnO_4$ and HIO_4/H_2SO_4 systems. Carbohydr Polym 117:247–254
24. Hu Y, Tang M (2015) Synthesis of starch-g-lactic acid copolymer with high grafting degree catalyzed by ammonia water. Carbohydr Polym 118:79–82
25. Zhu B, Ma D, Wang J, Zhang S (2015) Structure and properties of semi-interpenetrating network hydrogel based on starch. Carbohydr Polym 133:448–455
26. Selling G, Utt K, Finkenstadt V, Kim S, Biswas A (2015) Impact of solvent selection on graft co-polymerization of acrylamide onto starch. J Polym Environ 23(3):294–301
27. Naguib HF (2002) Chemically induced graft copolymerization of itaconic acid onto sisal fibers. J Polym Res 9(3):207–211
28. Sabaa MW, Mokhtar SM (2002) Chemically induced graft copolymerization of itaconic acid onto cellulose fibers. Polym Test 21(3):337–343
29. Işıklan N, Kurşun F, İnal M (2010) Graft copolymerization of itaconic acid onto sodium alginate using benzoyl peroxide. Carbohydr Polym 79(3):665–672
30. Milosavljević NB, Ristić MĐ, Perić-Grujić AA, Filipović JM, Štrbac SB, Rakočević ZL, Kalagasidis Krušić MT (2010) Hydrogel based on chitosan, itaconic acid and methacrylic acid as adsorbent of Cd^{2+} ions from aqueous solution. Chem Eng J 165(2):554–562
31. Lanthong P, Nuisin R, Kiatkamjornwong S (2006) Graft copolymerization, characterization, and degradation of cassava starch-g-acrylamide/itaconic acid superabsorbents. Carbohydr Polym 66(2):229–245
32. Xiao CM, Huang L (2013) Tailor-made starch-based gels bearing highly acidic groups. Starch-Starke 65(3–4):360–365
33. Soto D, Urdaneta J, Pernia K, Leon O, Munoz-Bonilla A, Fernandez-Garcia M (2015) Heavy metal (Cd^{2+}, Ni^{2+}, Pb^{2+} and Ni^{2+}) adsorption in aqueous solutions by oxidized starches. Polym Adv Technol 26(2):147–152
34. Soto D, Urdaneta J, Pernía K, León O, Muñoz-Bonilla A, Fernandez-García M (2015) Removal of heavy metal ions in water by starch esters. Starch-Stärke 67:1–10
35. Kiatkamjornwong S, Chomsaksakul W, Sonsuk M (2000) Radiation modification of water absorption of cassava starch by acrylic acid/acrylamide. Radiat Phys Chem 59(4):413–427
36. Hebeish A, El-Rafie MH, El-Sisi F, Abdel Hafiz S, Abdel-Rahman AA (1994) Oxidation of maize and rice starches using potassium permanganate with various reductants. Polym Degrad Stab 43(3):363–371
37. Hebeish A, Abd El-Thalouth I, El-Kashouti MA, Abdel-Fattah SH (1979) Graft copolymerization of acrylonitrile onto starch using potassium permanganate as initiator. Angew Makromol Chem 78(1):101–108
38. Zhang L-M, Chen D-Q (2001) Grafting of 2-(Dimethylamino)ethyl methacrylate onto potato starch using potassium permanganate/sulfuric acid initiation system. Starch-Stärke 53(7): 311–316
39. Zhang B, Zhou Y (2008) Synthesis and characterization of graft copolymers of ethyl acrylate/acrylamide mixtures onto starch. Polym Compos 29(5):506–510
40. Valls C, Rojas C, Pujadas G, Garcia-Vallve S, Mulero M (2012) Characterization of the activity and stability of amylase from saliva and detergent: laboratory practicals for studying the activity and stability of amylase from saliva and various commercial detergents. Biochem Mol Biol Educ 40(4):254–265
41. Chattopadhyay S, Singhal RS, Kulkarni PR (1997) Optimisation of conditions of synthesis of oxidised starch from corn and amaranth for use in film-forming applications. Carbohydr Polym 34(4):203–212
42. Mostafa KM (1995) Graft polymerization of methacrylic acid on starch and hydrolyzed starches. Polym Degrad Stab 50(2):189–194
43. Smith R (1967) Production and use of hypochlorite oxidized starches. Starch: chemistry and technology, vol 2. Academic Press, New York
44. Broido A (1969) A simple, sensitive graphical method of treating thermogravimetric analysis data. J Polym Sci Part A-2 Polym Phys 7(10):1761–1773
45. Kabiri K, Faraji-Dana S, Zohuriaan-Mehr MJ (2005) Novel sulfobetaine-sulfonic acid-contained superswelling hydrogels. Polym Adv Technol 16(9):659–666
46. Kabiri K, Omidian H, Zohuriaan-Mehr MJ, Doroudiani S (2011) Superabsorbent hydrogel composites and nanocomposites: a review. Polym Compos 32(2):277–289
47. Kizil R, Irudayaraj J, Seetharaman K (2002) Characterization of irradiated starches by using FT-Raman and FTIR spectroscopy. J Agric Food Chem 50(14):3912–3918
48. Cheetham NWH, Tao L (1998) Variation in crystalline type with amylose content in maize starch granules: an X-ray powder diffraction study. Carbohydr Polym 36(4):277–284
49. Xie W, Shao L, Liu Y (2010) Synthesis of starch esters in ionic liquids. J Appl Polym Sci 116(1):218–224
50. Zhang Y-R, Wang X-L, Zhao G-M, Wang Y-Z (2012) Preparation and properties of oxidized starch with high degree of oxidation. Carbohydr Polym 87(4):2554–2562
51. Nuñez-Santiago C, Garcia-Suarez FJL, Roman-Gutierrez AD, Bello-Pérez LA (2010) Effect of reagent type on the acetylation of barley and maize starches. Starch-Stärke 62(9):489–497
52. Xie W, Zhang Y, Liu Y (2011) Homogenous carboxymethylation of starch using 1-butyl-3-methylimidazolium chloride ionic liquid medium as a solvent. Carbohydr Polym 85(4):792–797
53. Zuo Y, Gu J, Yang L, Qiao Z, Tan H, Zhang Y (2013) Synthesis and characterization of maleic anhydride esterified corn starch by the dry method. Int J Biol Macromol 62:241–247

54. Chauhan GS, Kumar R, Verma M (2007) A study on the sorption of NO^{3-} and F^{-} on the carboxymethylated starch-based hydrogels loaded with Fe^{2+} ions. J Appl Polym Sci 106(3):1924–1931
55. Singh A, Nath L (2012) Synthesis, characterization, and compatibility study of acetylated starch with lamivudine. J Therm Anal Calorim 108(1):307–313
56. Cyras VP, Tolosa Zenklusen MC, Vazquez A (2006) Relationship between structure and properties of modified potato starch biodegradable films. J Appl Polym Sci 101(6):4313–4319
57. Lindeboom N, Chang PR, Tyler RT (2004) Analytical, biochemical and physicochemical aspects of starch granule size, with emphasis on small granule starches: a review. Starch-Stärke 56(3–4):89–99
58. Sandhu KS, Kaur M, Singh N, Lim S-T (2008) A comparison of native and oxidized normal and waxy corn starches: physicochemical, thermal, morphological and pasting properties. LWT-Food Sci Technol 41(6):1000–1010
59. Sujka M, Jamroz J (2009) α-Amylolysis of native potato and corn starches–SEM, AFM, nitrogen and iodine sorption investigations. LWT-Food Sci Technol 42(7):1219–1224
60. Gao Y, Wang L, Yue X, Xiong G, Wu W, Qiao Y, Liao L (2014) Physicochemical properties of lipase-catalyzed laurylation of corn starch. Starch-Stärke 66(5–6):450–456
61. Sánchez-Rivera MM, Flores-Ramírez I, Zamudio-Flores PB, González-Soto RA, Rodríguez-Ambríz SL, Bello-Pérez LA (2010) Acetylation of banana (Musa paradisiaca L.) and maize (Zea mays L.) starches using a microwave heating procedure and iodine as catalyst: partial characterization. Starch-Stärke 62:155–164
62. Mbougueng PD, Tenin D, Scher J, Tchiégang C (2012) Influence of acetylation on physicochemical, functional and thermal properties of potato and cassava starches. J Food Eng 108(2):320–326
63. Athawale VD, Lele V (2000) Thermal studies on granular maize starch and its graft copolymers with vinyl monomers. Starch-Stärke 52(6–7):205–213
64. Vasques CT, Domenech SC, Severgnini VLS, Belmonte LAO, Soldi MS, Barreto PLM, Soldi V (2007) Effect of thermal treatment on the stability and structure of maize starch cast films. Starch-Stärke 59(3–4):161–170
65. Dumitriu S (2004) Polysaccharides: structural diversity and functional versatility, 2nd edn. CRC Press, Boca Raton
66. Soliman AAA, El-Shinnawy NA, Mobarak F (1997) Thermal behaviour of starch and oxidized starch. Thermochim Acta 296(1–2):149–153
67. Afolabi TA (2012) Synthesis and physicochemical properties of carboxymethylated bambara groundnut (Voandzeia subterranean) starch. Int J Food Sci Technol 47(3):445–451
68. Krušić MK, Filipović J (2006) Copolymer hydrogels based on N-isopropylacrylamide and itaconic acid. Polymer 47(1):148–155
69. Díez-Peña E, Quijada-Garrido I, Barrales-Rienda JM (2003) Analysis of the swelling dynamics of cross-linked P(N-iPAAm-co-MAA) copolymers and their homopolymers under acidic medium. A kinetics interpretation of the overshooting effect. Macromolecules 36(7):2475–2483. doi:10.1021/ma021469c
70. Yin Y, Ji X, Dong H, Ying Y, Zheng H (2008) Study of the swelling dynamics with overshooting effect of hydrogels based on sodium alginate-g-acrylic acid. Carbohydr Polym 71(4):682–689
71. Valencia J, Piérola IF (2002) Swelling kinetics of poly(N-vinylimidazole-co-sodium styrenesulfonate) hydrogels. J Appl Polym Sci 83(1):191–200
72. Díez-Peña E, Quijada-Garrido I, Barrales-Rienda JM (2002) Hydrogen-bonding effects on the dynamic swelling of P(N-iPAAm-co-MAA) copolymers. A case of autocatalytic swelling kinetics. Macromolecules 35(23):8882–8888
73. Kapusniak J, Siemion P (2007) Thermal reactions of starch with long-chain unsaturated fatty acids. Part 2. Linoleic acid. J Food Eng 78(1):323–332
74. Bhandari PN, Singhal RS (2002) Studies on the optimisation of preparation of succinate derivatives from corn and amaranth starches. Carbohydr Polym 47(3):277–283
75. Richter A, Paschew G, Klatt S, Lienig J, Arndt K-F, Adler H-J (2008) Review on hydrogel-based pH sensors and microsensors. Sensors 8(1):561–581
76. Jain CK, Singhal DC, Sharma MK (2004) Adsorption of zinc on bed sediment of River Hindon: adsorption models and kinetics. J Hazard Mater 114(1–3):231–239
77. Prasad MNV, Freitas H (2000) Removal of toxic metals from solution by leaf, stem and root phytomass of Quercus ilex L. (holly oak). Environ Pollut 110(2):277–283
78. Shukla SR, Pai RS (2005) Adsorption of Cu(II), Ni(II) and Zn(II) on dye loaded groundnut shells and sawdust. Sep Purif Technol 43(1):1–8
79. Orozco-Guareño E, Santiago-Gutiérrez F, Morán-Quiroz JL, Hernandez-Olmos SL, Soto V, Wdl Cruz, Manríquez R, Gomez-Salazar S (2010) Removal of Cu(II) ions from aqueous streams using poly(acrylic acid-co-acrylamide) hydrogels. J Colloid Interface Sci 349(2):583–593
80. Quintana JR, Valderruten NE, Katime I (1999) Synthesis and swelling kinetics of poly(Dimethylaminoethyl acrylate methyl chloride quaternary-co-itaconic acid) hydrogels. Langmuir 15(14):4728–4730
81. Jeon C, Höll WH (2004) Application of the surface complexation model to heavy metal sorption equilibria onto aminated chitosan. Hydrometallurgy 71(3–4):421–428
82. Plazinski W, Dziuba J, Rudzinski W (2013) Modeling of sorption kinetics: the pseudo-second order equation and the sorbate intraparticle diffusivity. Adsorption 19(5):1055–1064